Beamline 9.3.1

Atomic, Molecular, and Materials Science

Beamline 9.3.1: Monochromator upgrade

Schlachter, A.S., R. Weidenbach, E. Domning, W. Steele, T. Miller, C. Hernikl, T. Warwick

Resonant x-ray fluorescence holography: Three-dimensional atomic imaging in true color

Omori, S., L. Zhao, S. Marchesini, M. A. Van Hove, C. S. Fadley

Shallow and deep core level ionic fragmentation of the CCl_4 molecule

Santos, A.C.F., J.B. Maciel, M.M. Sant' Anna, K.T. Lung, J. Cotter, W. Stolte, G.G.B. de Souza

XANES spectroscopy of Ti and V centers grafted onto mesoporous sieves: Preliminary results

Lin, W., D. Bruehwiler, H. Frei

Beamline 9.3.1:
Monochromator Upgrade

Fred Schlachter, Richard Weidenbach, Ed Domning, William Steele, Tom Miller,
Chris Hernikl, and Tony Warwick[1]
[1]Advanced Light Source, Ernest Orlando Lawrence Berkeley National Laboratory,
University of California, Berkeley, California 94720, USA

INTRODUCTION

A double-crystal monochromator is installed on bend-magnet beamline 9.3.1. It is designed to provide photons in the energy range 2.3 to 5.5 keV. Although it has successfully operated for energy scans over limited energy ranges, it has generally not been used for applications requiring scans over a large energy range, e.g., for EXAFS. The monochromator has been redesigned and rebuilt for improved performance. The upgraded monochromator shows improved thermal and mechanical stability, and energy scans over large energy ranges are now possible. A new control system and user interface are being implemented. The beamline is now ready for users.

ISSUES

The performance of the monochromator as designed was limited by several factors.

- thermal stability due to insufficient cooling of the first crystal;
- mechanical stability of the crystal mounts;
- lack of position readouts of crystal adjustments;
- outdated and undocumented control system.

The primary limitation of the monochromator is that the first crystal absorbs significant heat, resulting in thermal expansion and an increase of d-spacing of the crystal. This effect, before cooling was implemented, was time and photon-energy dependent, and limited both scanning range and stability of beam position and intensity with time. A second limitation was mechanical stability of the crystal mounts, and coupling of crystal motions (theta and chi angles). Picomotors were used to control theta and chi adjustments inside the vacuum, but, without position readouts, it was easy to get lost, resulting in tuning difficulties and unforgiving operation. Finally, the control system was essentially non-commercial and undocumented, and the LabView code was not documented, resulting of difficulties in upgrading the equipment and/or the operating system.

IMPROVEMENTS

The ground rule for upgrading the monochromator was to preserve the mechanical linkage (the "boomerang") which controls the position and angle of the two crystals in the monochromator.

The crystal mounts were totally re-engineered. The primary improvement was to add water cooling to the first crystal. This was achieved by circulating chilled temperature-controlled water

through a copper plate which is part of the mount for the first crystal. Indium foil and a gallium eutectic are the heat-transfer media to cool the first crystal.

The support arrangement for each rotation axis of the crystal mounts was changed from a single flexural hinge to a pair of flexural hinges, providing considerably improved mechanical stability and isolation of theta and chi motions.

Theta and chi coarse adjustments are made, as before, by picomotors in vacuum. However, a piezo actuator has been added in series with the picomotor for adjustment of theta (theta puts the second crystal on the Bragg peak of the first crystal) for eventual feedback on either photon beam intensity or vertical beam position (which are coupled). Provision has been made for installing a piezo actuator for adjustment of chi (left-right tilt adjustment of the second crystal) should fine adjustment and/or feedback on horizontal beam position be required.

LVDTs (Linear Variable Differential Transformers) were installed to measure theta and chi position. These allow computer control of theta and chi, feedback, and maintaining reference positions. The beamline is now easy to tune and control.

The LabView code running the control and data-acquisition systems has been entirely rewritten, keeping the flavor of the previous code while adding new features, making operation of the beamline more user friendly, and having a maintainable code. New counting cards add additional counting channels.

Many improvements were made to mechanical parts of the boomerang and crystal mounts, primarily in the selection of materials to provide smooth long-term operation and to minimize galling and other maintenance issues. The rotary parts of the mechanisms were redesigned and rebuilt as needed.

OPERATION and TESTING

Energy repeatability is of concern to users when multiple scans are made over the same energy range. The method used previously was to remove backlash from the mechanism by selecting a low energy, then increasing the energy to the starting point of the scan. Motor steps were counted to determine energy. A tilt sensor was used to “home” the motor from time to time. We found that motor steps are not a reliable method for determining photon energy. For example, a series of measurements of photoabsorption in argon gas had the peak spread over greater than 1 eV, with a mean spread of nearly 0.4 eV. The tilt sensor, previously used for homing only, was at least a factor of two better (see Fig. 1). We are thus using the tilt sensor to measure photon energy, pending installation of a rotary encoder for installation on the rotation axis of the first crystal. This will provide improved energy repeatability.

Tests are underway on beam size and beam-position stability. Initial results show a beam of less than 1-mm diameter, with beam position stability of +/- two mm in scans over a range of 2000 eV. Flux is relatively constant in scans over a large energy range (see Fig. 2).

Energy calibration has been accomplished using photoabsorption and photoemission measurements.

The new user interface is integrated with the new control system, and is presently undergoing testing. It is being phased in as new functions become available.

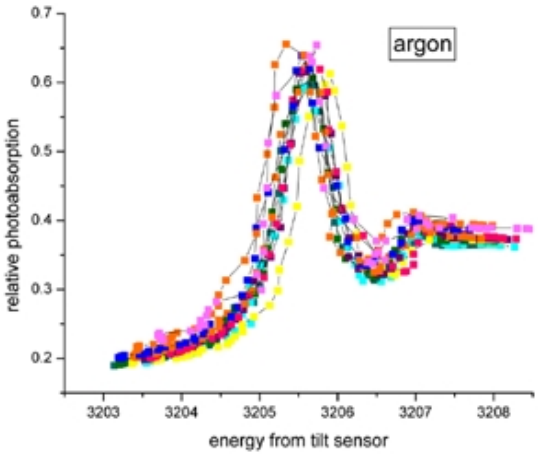

Figure 1. Relative photoabsorption in argon gas as a function of photon energy (eV) as measured by the tilt sensor. Multiple scans are shown to indicate repeatability.

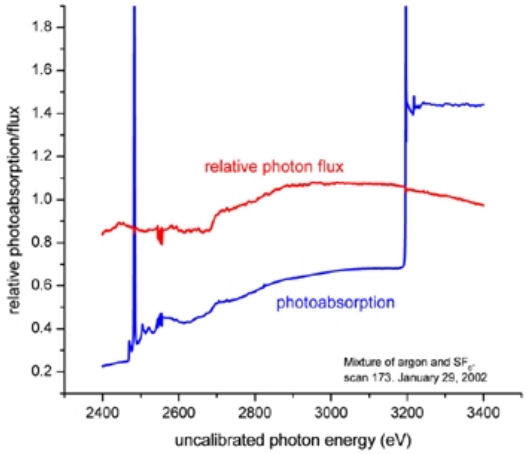

Figure 2. Relative photoabsorption and photon flux for a mixture of argon and SF_6 gases. Scan was made continuously with no adjustments.

OUTLOOK

We expect beamline 9.3.1 to operate with greatly improved stability and ease, and greater scanning range than was previously possible. It is a very useful beamline for K-shell studies on elements from sulfur through vanadium, and for L-shell and M-shell work on elements with electron binding energies in the range 2300 to 5500 eV.

ACKNOWLEDGMENTS

We thank Alastair MacDowell, Dennis Lindle, Will Thur, and Wayne Stolte for their kind assistance to this project.

This work was supported by the Director, Office of Energy Research, Office of Basic Energy Sciences, Materials Science Division, of the U.S. Department of Energy under Contract No. DE-AC03-76SF00098.

Principal investigator: Fred Schlachter, Advanced Light Source, Ernest Orlando Lawrence Berkeley National Laboratory. Email: fsschlachter@lbl.gov. Telephone: 510-486-4892.

Resonant X-ray Fluorescence Holography: Three-Dimensional Atomic Imaging in True Color

S. Omori[1,2,#], L. Zhao[1,3], S. Marchesini[1], M. A. Van Hove[1,3,4], and C. S. Fadley[1,3]

[1] Materials Sciences Division, Lawrence Berkeley National Laboratory, Berkeley, California 94720
[2] Institute of Industrial Science, University of Tokyo, Tokyo 153-8505, Japan
[3] Department of Physics, University of California, Davis, California 95616
[4] Advanced Light Source, Lawrence Berkeley National Laboratory, Berkeley, California 94720
[#]Present address: Sony Research, Kawasaki, Japan

X-ray fluorescence holography (XFH) is a relatively new experimental tool for directly determining the local three-dimensional atomic structure around a given type of atom [1-4]. This element-specific method is based on the same concept as photoelectron holography [5], but detects instead fluorescent x-ray photons.

In the first type of XFH to be demonstrated experimentally [1a], one measures the interference between the fluorescent radiation directly emitted by the excited atoms and additional wave components of the same radiation scattered by various near-neighbor atoms. It is thus necessary to measure a given fluorescent intensity as a function of the direction of emission over as large a solid angle as possible. This method, for which the fluorescent atoms inside the sample act as sources and the intensity is measured in the far field, has been termed normal x-ray fluorescence holography (XFH) [2] or more specifically "direct XFH". In parallel with the first direct XFH experiment, Gog et al. [2a] proposed and demonstrated a different approach (termed multiple energy x-ray holography (MEXH) or "inverse XFH") by applying the optical reciprocity principle and exchanging the roles of source and detector. In this case, the fluorescent atoms inside the sample become the detectors for the net field produced by the interference of the incident x-ray beam and the components of this beam that are scattered by near-neighbor atoms. With present detection systems, MEXH is faster, as the incident beam can be very intense (e.g. emitted directly from a beamline monochromator or an undulator harmonic), and one can furthermore in principle detect all of the fluorescence emitted above the sample surface. Here, one is thus measuring the total fluorescence yield of a given atomic transition as a function of the direction of the incident x-ray beam. Being able to measure at multiple energies also results in images with less aberration due to twin-image effects and other non-idealities [2,5,6]. Recent XFH/MEXH studies have demonstrated the ability to image a first-row element in the presence of a transition metal [3], and to study the local atomic environment in a quasicrystal, even though translational periodicity is lacking for such a system [4]. Current experiments are by and large detector-limited as to the speed of data acquisition. In the ALS Compendium of 2000, we have discussed a project that has successfully measured the first MEXH holograms and holographic atomic images at the ALS [7].

Even though XFH and MEXH in their current formulations offer powerful methods to probe the local atomic structure around a given atom, there still remains one deficiency: the techniques may be element-specific for the central fluorescing atom in the structure (a quality they share with extended x-ray absorption fine structure (EXAFS)), but there is no simple way to determine the

near-neighbor atomic identities. Use can be made of the differences in non-resonant x-ray scattering strengths between different atoms (as is done with differences in electron scattering strength in EXAFS), but this is only unambiguous when atomic numbers are relatively far apart, as recently illustrated for the case of O and Ni in NiO [3]. In the present work, we propose a significant improvement to MEXH, resonant x-ray fluorescence holography (RXFH), that should enable the direct discrimination of different atoms in reconstructed images, even for the most difficult cases where atomic numbers of elements involved are very close together. It is in this sense that we can finally speak of atomic images "in true color" [8].

The principle of RXFH is discussed here for the example of a binary compound of AB_3 type with close atomic numbers, specifically $FeNi_3$, for which $Z_{Ni} - Z_{Fe} = 2$ and the fractional change in atomic number is only ~0.08 [8]. The central fluorescing atom of the reconstructed images is always chosen to be atom *A* (Fe in this case), and the anomalous dispersion associated with an absorption edge for element *B* (Ni in this case) is used to selectively image atoms *B* surrounding the central atom. In the usual implementations of MEXH in which both atoms *A* and *B* are to be equally imaged, the incident x-ray energies *E* are usually chosen in such a way that they are close enough to E_{abs}^{A}, the absorption edge of element *A*, for the efficient excitation of fluorescent x-rays from *A*, but also far enough from both E_{abs}^{A} and any edges E_{abs}^{B} of atom B that the anomalous dispersion terms in the x-ray scattering factors for *A* and *B* are not significant. In RXFH, by contrast, we will choose several *E*'s in the vicinity of an absorption edge E_{abs}^{B} of element *B*. The basic idea here is thus similar to that of multiple-wavelength anomalous diffraction (MAD) for phase determinations in conventional x-ray diffraction studies, but with the significant difference that there is from the outset no phase uncertainty in MEXH.

Making use of experimentally determined x-ray scattering factors for Fe (non-resonant) and Ni (resonant), as shown in Fig. 1, we have thus theoretically simulated holograms [6b] for a large cluster of atoms representing the $FeNi_3$ lattice as the Fe Kα fluorescence at 6.4 keV is monitored while scanning through the Ni K edge at about 8.3 keV [8]. As a first trial set of data, we have finally obtained MEXH and RXFH images based on the three energies shown in Fig. 2: below, on, and above the Ni K edge. One promising procedure for imaging in RXFH is shown elsewhere [8] to be using two difference holograms for E_1-E_2 and (with reversed sign) E_3-E_2. Fig. 2 shows the $FeNi_3$ crystal structure, together with normal MEXH images and RXFH images from these difference holograms. Fig. 2 makes it clear that the Ni-atom images are strongly suppressed in the RXFH images, thus suggesting this as a new approach in x-ray fluorescence holography for identifying near-neighbor atoms to a given type of fluorescent emitter.

In conclusion, resonant x-ray fluorescence holography should make it possible to obtain additional information on near-neighbor chemical identities that would lead to a much more complete structural characterization of any system, particularly one in which possible compositional disorder on the nm scale is present, and thus to a much broader applicability for nanoscale materials characterization. Future experiments at the ALS will explore this approach experimentally.

REFERENCES

[1] (a) M. Tegze, G. Faigel, Nature 380 (1996) 49; (b) (b) G. Faigel and M. Tegze, *Rep. Prog. Phys.* **62** (1999) 355.

[2] (a) T. Gog, P.M. Len, G. Materlik, D. Bahr, C.S. Fadley, C. Sanchez-Hanke, Phys. Rev. Lett. **76** (1996) 3132; (b) P.M. Len, C.S. Fadley, and G. Materlik, in X-ray and Inner-Shell Processes: 17th International Conference, R.L. Johnson, H. Schmidt-Böcking, and B.F. Sonntag, Eds., AIP Conference Proceedings, No. 389 (AIP, New York, 1997) p. 295.
[3] M. Tegze, G. Faigel, S. Marchesini, M. Belakhovsky, O. Ulrich, Nature 407, (2000) 38.
[4] S. Marchesini, et al., Phys. Rev. Lett. 85, (2000), 4723-6
[5] G.R. Harp, D.K. Saldin, B.P. Tonner, Phys. Rev. Lett. 65 (1990) 1012; plus more recent work at the ALS by P.M. Len et al. Phys. Rev. B **59** (1999) 5857
[6] (a) P.M Len, Ph.D. thesis, University of California at Davis (1997) and (b) simulation and imaging software described at http://electron.lbl.gov/holopack/holopack.html.
[7] S. Marchesini, L.Zhao, L. Fabris, M. W. West, J. Bucher, D. K. Shuh, W. C. Stolte, M. J. Press , A.S. Schlachter, Z. Hussain, and C. S. Fadley, ALS Compendium of Abstracts 2000: http://alspubs.lbl.gov/AbstractManager/uploads/00135.pdf.
[8] S. Omori, L. Zhao, S. Marchesini, M.A. Van Hove, and C.S. Fadley, Phys. Rev. B **65** (2002) 014106.

This work was supported by the U.S. Department of Energy, Office of Science, Office of Basic Energy Sciences, Materials Sciences Division, under Contract No. DE-AC03-76SF00098..

Principal investigator: Stefano Marchesini, Materials Sciences Division, Lawrence Berkeley National Laboratory. Email: marchesini@lbl.gov. Telephone: 510-486-4581.

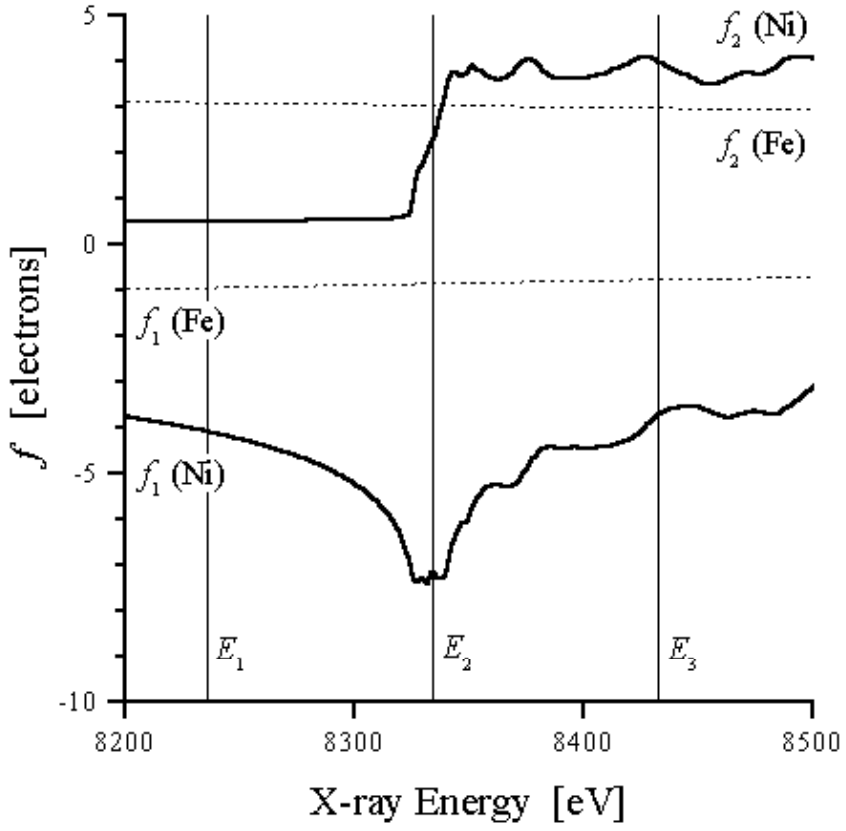

Fig. 1-- The atomic x-ray scattering factors f_1 and f_2 for Fe (dotted lines) and Ni (solid lines) as a function of x-ray energy around the *K* edge of Ni. The overall scattering factor is given by $f_{Atom} = f_0(\theta) + f_1 - if_2$, with $f_0(\theta)$ the form factor. The three energies used for the simulations of E_1, E_2 and E_3 are indicated by vertical solid lines and correspond to 8235 eV, 8334 eV, and 8433 eV, respectively.

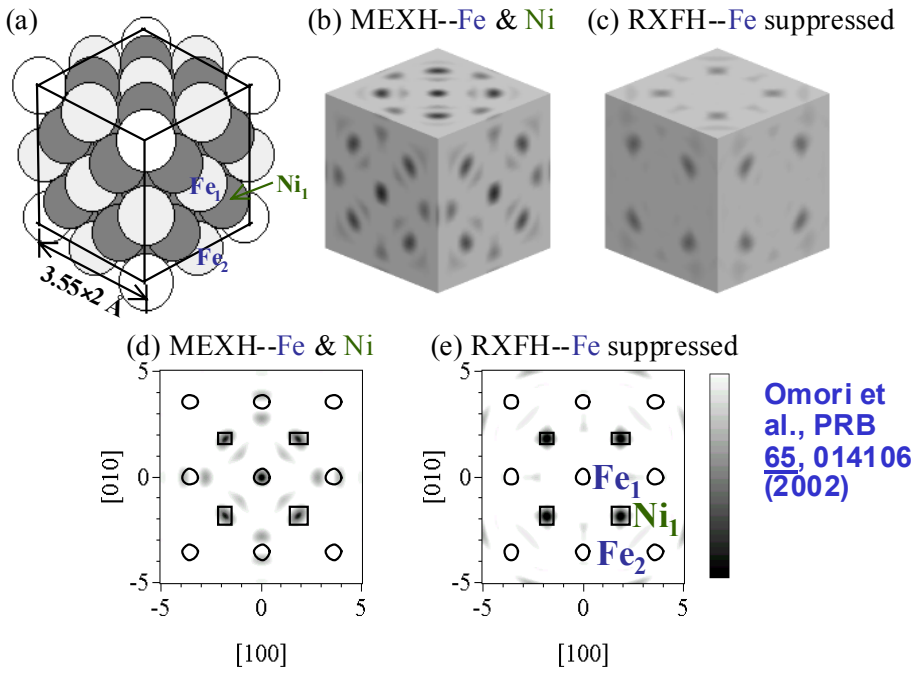

Fig. 2-- Comparison of multi-energy inverse x-ray fluorescence holographic images based on the negative of the real part of images generated using both the standard inversion algorithm (MEXH) and resonant holography (RXFH) based on two difference images (E_1-E_2 and E_3-E_2). These images are based on single-scattering cluster simulations of holograms [6b] at the three energies E_1, E_2 and E_3 for an $FeNi_3$ crystal containing about 10,000 atoms. (a) Near-neighbor atomic model of $FeNi_3$ for comparison to the reconstructed images in (b) and (c) and including 8 unit cells with the lattice constant of 3.55 Å. Fe atoms are lighter gray, and Ni atoms darker gray. The unique types of Fe and Ni atoms observed in (b) are labelled as Fe_1, Fe_2 and Ni_1. (b) Three dimensional reconstructed image from MEXH in cross section along six {001} planes. (c) Corresponding image from RXFH. The fluorescing Fe atom is located at the centers of the cubes in (a), (b) and (c). (d) Enlarged reconstructed image from MEXH in the (001) plane. (e) Corresponding enlarged image from RXFH. The true atomic positions of Fe and Ni atoms are shown as circles and squares, respectively, and certain key atomic positions are also labelled.

SHALLOW AND DEEP CORE LEVEL IONIC FRAGMENTATION OF THE CCl_4 MOLECULE

A. C. F. Santos[1] , J. B. Maciel[1] , M. M. Sant'Anna[2], K. T. Lung[4] , J. Cotter [5], W. Stolte[3] , and G. G. B. de Souza[1]

[1]Instituto de Química, Universidade Federal do Rio de Janeiro, Brazil
[2]Pontifícia Universidade Católica do Rio de Janeiro, Brazil
[3]Advanced Light Source, Berkeley, CA, USA
[4]University of Waterloo, Canada
[5]University of Nevada, Reno, USA

Carbon tetrachloride, CCl_4, is a volatile compound with several important technological applications, being for instance used as an etching agent in microelectronics. In addition, the CCl_4 molecule pollutes atmosphere harmfully and has been related to the so-called greenhouse effect [4]. Several studies have been dedicated to the photoabsorption spectrum of the CCl_4 molecule, both in the valence and inner-shell regions [1-4]. This molecule presents a tetrahedral symmetry (T_d point group).

In this work we report on the ionic fragmentation of the CCl_4 molecule following valence, and core level photoexcitation, using tunable synchrotron radiation as exciting source. Branching ratios for the ionic fragments have been determined, as a function of the incident photon energy around the valence, Cl 2*p* edge (~200 eV)., C 1*s* continuum (~ 300 eV), and Cl 1s (~ 2800 eV) regions.

The valence and shallow core levels (Cl 2p and C 1s) measurements were performed at the Center for Advanced Microstructures and Devices (CAMD), Louisiana, USA. The experimental set up has been described recently [5]. Basically, light from a toroidal grating monochromator (TGM) beamline intersected an effusive gaseous sample inside a high vacuum chamber, with base pressure in the 10^{-8} torr range. PEPICO and PIPICO data were determined as a function of the photon energy using a time-of-flight mass spectrometer.

The second part of this work (deep core level ionization) was performed using x-ray synchrotron radiation from beamline 9.3.1 at the Advanced Light Source (ALS) in Berkeley, California. 9.3.1 is a bending magnet beamline covering 2-6 keV photon-energy range. This beamline provides a flux of 10^{11} photons s^{-1} in a bandpass $\leq$ 0.5 eV. Photon-energy calibration was achieved by scanning the monochromator through the Cl K-edge region while monitoring the total-ion yield . The photon-energy was determined with 0.2 eV accuracy. Figs. 1 and 2 show the PEPICO mass spectra of CCl_4 around the Cl 2p and Cl 1s edges.

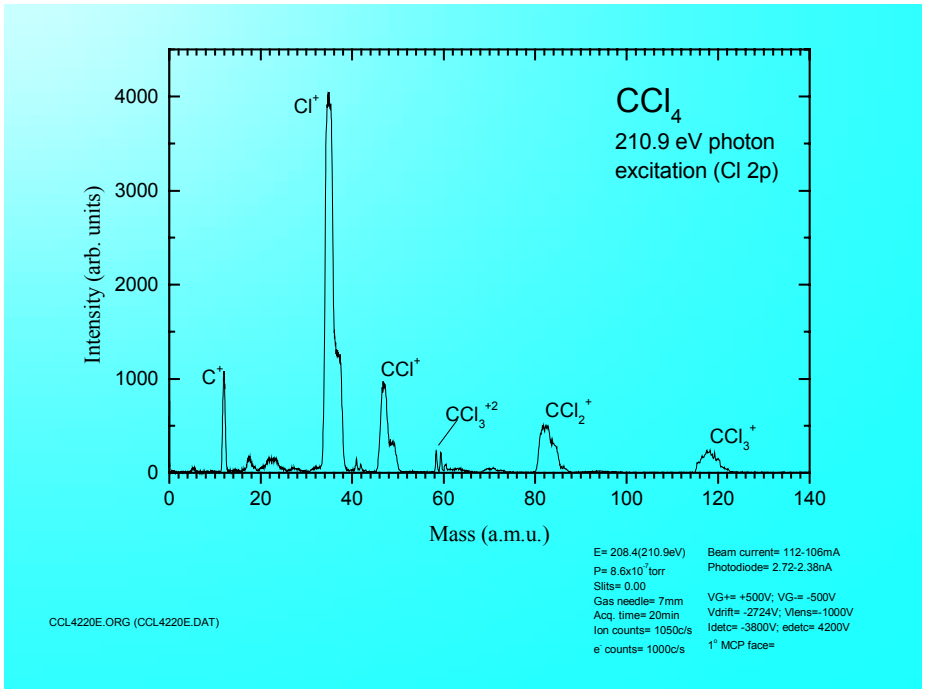

Fig 1. - Mass Spectrum of CCl_4 molecule near the Cl 2p edge (210 eV).

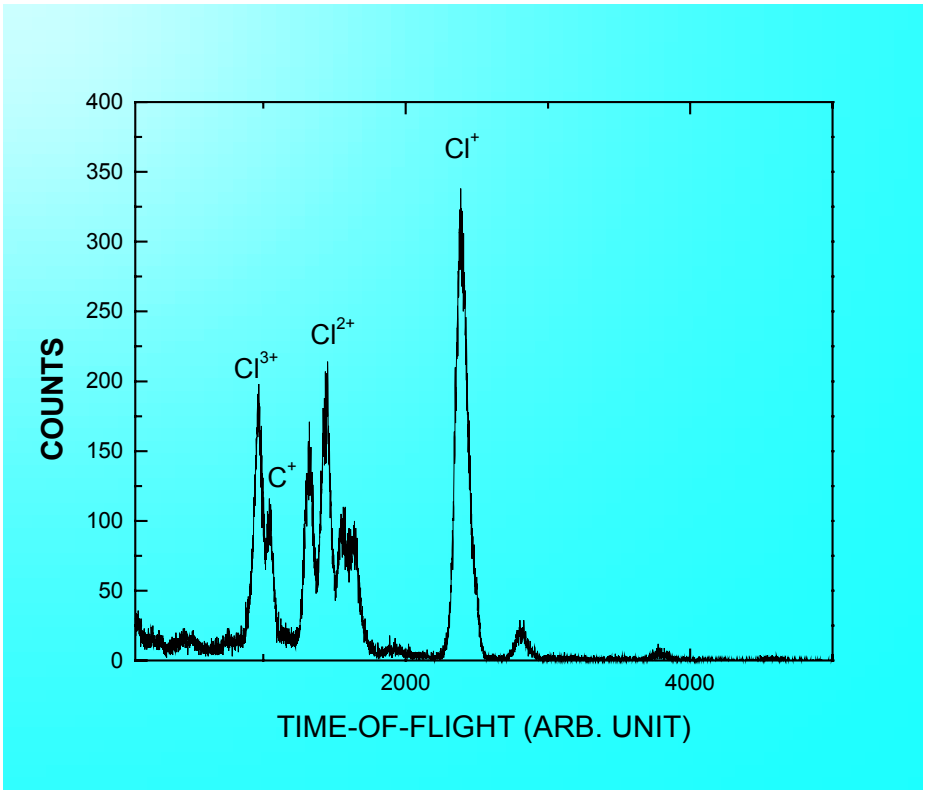

Fig.2 – Mass spectrum of CCl_4 molecule around Cl 1s edge.

There is no evidence for stable CCl_4^+ ion in the energy range studied in this work in accordance with earlier studies using electron impact technique [6, 7]. The first evidence for metastable CCl_4^+ ion was given by Drewello *et al.* [8], with lifetimes in the order of 10^{-5} s. According to Kaufmann *et al.* [8], the CCl_4^+ is not observed because the excitation of the carbon tetrachlorine molecule occurs into a repulse excited state of neutral CCl_4 which dissociates into Cl and CCl_3 that in turns, autoionizes giving rise to CCl_3^+ ion. Leiter *et. al.* [6] observed the metastable dissociation of CCl_4^{+*} into CCl_3^+ and Cl, avoiding the postulation of dissociation of neutral CCl_4 prior to ionization.

The authors would like to thank the CAMD and ALS staffs for the very efficient operation of the respective synchrotron rings. They also would like to express their gratitute to Prof. Fred Schlater (ALS) and C. Cisneros (UNAM) for support. We also acknowledge Prof. D. Lindle for the use of a vacuum chamber. Three of the authors (A.C.F.S., J.B.M. and G.G.B.de S.) are indebted to FAPERJ and CNPq (Brazil) for financial assistance.

References:

1 – A. P. Hitchcock and C. E. Brion, Journ. Electr. Spectr. Rel. Phen., **14** (1978) 417-441.
2 – W. Zhang, T. Ibuki, and C. E. Brion, Chem. Phys. **160** (1992) 435-450.
3 – G. O'Sullivan, J. Phys. B. At. Mol. Opt. Phys. **15** (1982) 2385-2390.
4– G. R. Burton, W. F. Chan, G. Cooper and C. E. Brion Chem. Phys. **181** (1994) 147-172.
5- A.C.F. dos Santos, C.A.Lucas and G.G.B. de Souza, J.El.Spectr. and Rel. Phen., **114-116** (2001) 115-121.
6- K. Leiter, K. Stephan, E. Märk, and T. D. Märk, Plasma Chemistry and Plasma Processing, **4**, (1984) 235-249.
7- R. F. Baker and J. T. Tate, Phys. Rev. **53**, 683 (1938).
8- T. Drewello, T. Weiske, and H. Schwarz, Angew. Chem. Int. Ed. Engl. **24,** 869 (1985).

Principal investigator: Gerardo Gerson B de Souza, Instituto de Química, Universidade Federal do Rio de Janeiro. E-mail: gerson@iq.ufrj.br. Telephone: (55) 021 2590-9024.

XANES Spectroscopy of Ti and V Centers Grafted onto Mesoporous Sieves: Preliminary Results

W. Lin, D. Bruehwiler, and H. Frei

Physical Biosciences Division, Lawrence Berkeley National Laboratory, Berkeley, CA 94720

INTRODUCTION

Photochemical synthesis of a fuel by reduction of CO_2 using visible light as energy source and H_2O as electron source is one of the most attractive, yet unrealized goals in solar energy to fuel conversion. Photosynthesis of methanol for large scale use in fuel cells is considered a promising option for the replacement of fossil fuel combustion as a means of power generation. We are exploring photochemistry at the gas-solid interface of transition metal molecular sieves as a method for CO_2 conversion to methanol. A most critical aspect of this task is the reliable characterization of the framework of grafted metal centers in these materials, and the verification of the structural integrity of the photoreactor under use. X-ray absorption techniques, especially EXAFS (Extended X-Ray Absorption Fine Structure) and XANES (X-Ray Absorption Near Edge Structure) spectroscopy are the best tools for this type of solids. Based on earlier pre-edge X-ray absorption characterization of Ti silicalite materials at ALS beamline 9.3.1, we have recently been able to establish for the first time some of the key intermediates of carbon oxide reduction and H_2O_2 interaction in this molecular sieve.[1-3]

In an effort to push the redox response of the metal centers from the UV towards visible photon energies, we are exploring the possibility of incorporating visible light-absorbing multinuclear assemblies into molecular sieves. A first step in the synthesis of such assemblies is the introduction of an anchor metal into the material in the form of a framework or grafted center. We have prepared grafted and framework Ti and V centers in mesoporous silicate sieves and have begun structural characterization of the materials by pre-edge absorption spectroscopy.

RESULTS

Using a specially designed sample holder for recording spectra of up to 12 molecular sieve samples in the form of pressed wafers in transmission or fluorescence mode, we have begun to record framework and grafted TiMCM41 and VMCM41 materials synthesized in our laboratory. As described by F. Schlachter in the ALS 2001 Compendium paper " Beamline 9.3.1: Monochromator Upgrade", the beam stability has been greatly improved since our earlier measurements. The new performance allows us to conduct reproducible scans over an energy range of several hundred eV, as demonstrated in Figure 1 by a 500 eV scan covering the Ti K-edge and the Ba L_3-edge of $BaTiO_3$. The spectrum shows the result of a single scan. The sample was a pressed wafer (diameter 1 cm, thickness 100 micron) of $BaTiO_3$ crystallites embedded in a silicate matrix. The measurement was conducted in transmission mode using a Si photodiode detector (Hamamatsu model S2744-08).

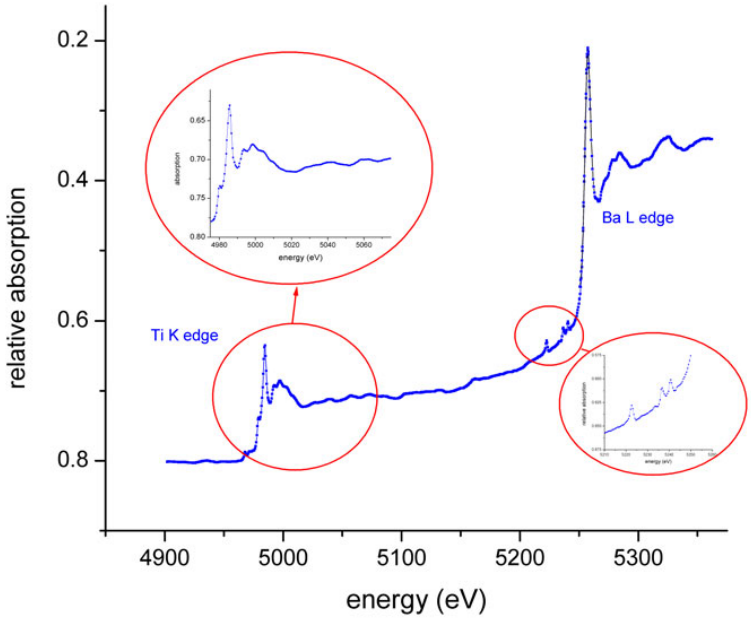

Figure 1. X-ray-absorption spectrum of crystalline barium titanate.

Figure 2a shows the absorption spectrum of framework TiMCM41 sieve in which 1 percent of the Si atoms are isomorphically substituted by Ti. Since the framework sites are tetrahedrally coordinated by oxygen, Ti in such sites gives rise to a sharp 1s-3d transition (A_1-T_2 component) absorbing around 4970 eV. By contrast, any extraframework TiO_2 clusters would feature octahedrally coordinated Ti that only contributes to the K-edge absorption but not to the pre-edge peak (optically forbidden). Figure 2a shows that the intensity of the 1s-3d peak relative to the height of the plateau between K-edge and the onset of the extended region is greater than 0.7. This is indicative of 100 percent framework substitution of the Ti, with no extraframework Ti oxide clusters present in the pores.

Similarly, the pre-edge peak of the grafted TiMCM41 spectrum shown in trace b of Figure 2 indicates that at least 90 percent of the Ti is in tetrahedral coordination. Diffuse reflectance UV and transmission FT-IR spectra of the material imply that the tetrahedrally coordinated Ti centers are tripodal (Si-O)TiOH moieties, i.e., the Ti is covalently anchored to three Si centers on the surface of the pore. Next, measurements will be conducted on recently prepared grafted VMCM materials.

These preliminary measurements establish the high degree of covalent anchoring of Ti as isolated centers in our mesoporous silicate materials. The quality of the single scan results displayed in Figure 1 and 2 shows that the recent monochromator upgrade at beamline 9.3.1 opens up routine XANES and EXAFS measurements up to energies of 5500 eV.

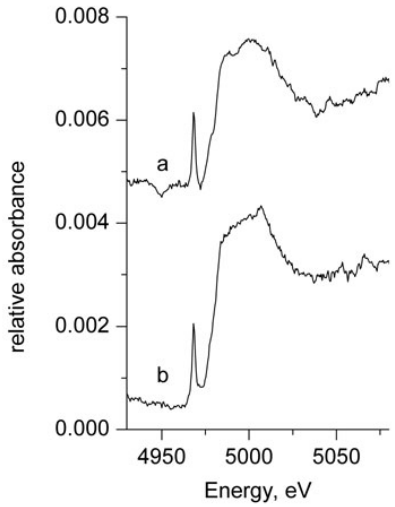

Figure 2. XANES spectrum of framework-substituted Ti-MCM41 (a), and grafted Ti-MCM41 (b).

REFERENCES

1. N. Ulagappan and H. Frei, "Mechanistic Study of CO_2 Photoreduction in TS-1 Molecular Sieve". *J. Phys. Chem. A* **104**, 7834 (2000).
2. Y.H. Yeom and H. Frei, "Photoactivation of CO in Ti Silicalite Molecular Sieve". *J. Phys. Chem. A* **105**, 5334 (2001).
3. W. Lin and H. Frei, "Photochemical and FT-IR Probing of the Active Site of Hydrogen Peroxide in Ti Silicalite Sieve". *J. Am. Chem. Soc*., submitted.

This work was supported by the Director, Office of Science, of the U.S. Department of Energy under Contract No. DE-AC03-76SF00098. The authors thank Fred Schlachter for assistance in the experiments.

Principal Investigator: Heinz Frei, Physical Biosciences Division, Lawrence Berkeley National Laboratory. E-mail: HMFrei@lbl.gov Telephone: 510-486-4325